Article

Discovery Medicine 2025; 37(194): 563–572
https://doi.org/10.24976/Discov.Med.202537194.48

Regulating Osteogenic Fate: How Dexamethasone Targets the CAST-CAPN1-ATP5A1 Axis in BMSCs

Gang Zhong[1,2], Shiqiang Cen[1,2], Zhou Zhong[1,2], Lin Teng[3,*]

[1]Department of Orthopedic Surgery, West China Hospital, Sichuan University, 610041 Chengdu, Sichuan, China
[2]Trauma Center, West China Hospital, Sichuan University, 610041 Chengdu, Sichuan, China
[3]Department of Orthopedics, West China Airport Hospital, Sichuan University, The First People's Hospital in Shuangliu District, 610200 Chengdu, Sichuan, China
*Correspondence: tenglin_ttlin@163.com (Lin Teng)
Published: 20 March 2025

Background: Osteoporosis is a common systemic metabolic disease, leading to increased bone fragility and risk of fractures. Research has shown that Adenosine triphosphate (ATP) synthase, H+transporting, mitochondrial F1 complex, alpha subunit 1 (ATP5A1), a crucial component in ATP production, is inhibited in dexamethasone (DEX)-induced osteoblasts. Therefore, this study aimed to investigate the molecular mechanism underlying the inhibitory impact of DEX on osteogenic differentiation in rat bone marrow mesenchymal stem cells (BMSCs).

Methods: Rat BMSCs were treated with varying concentrations of DEX for 14 days, followed by subsequent analyses. The expression levels of calpastatin (CAST), calpain 1 (CAPN1), and ATP5A1 were assessed using quantitative reverse transcription polymerase chain reaction (qRT-PCR) and Western blotting analyses. Furthermore, osteogenic marker proteins and ATP activity were evaluated employing Western blotting analysis and enzyme-linked immunosorbent assay (ELISA). Moreover, to determine the regulatory role of DEX on the CAST-CAPN1 axis, overexpression plasmids for *CAST* (oe-*CAST*) and *CAPN1* (oe-*CAPN1*) were constructed. Additionally, osteogenic differentiation and ATP activity in BMSCs were analyzed using qRT-PCR, Western blotting, Alizarin Red S staining, and ELISA.

Results: With increasing concentrations of DEX, the expression of the CAST-CAPN1-ATP5A1 axis in BMSCs was significantly altered ($p < 0.05$). DEX downregulated the levels of osteogenic markers, including Runt-Related Transcription Factor 2 (RUNX2), alkaline phosphatase (ALP), and osteopontin (OPN), while reducing ATP activity ($p < 0.05$). However, oe-*CAST* partially mitigated the inhibitory effects of DEX on osteogenic differentiation and ATP activity ($p < 0.05$). In contrast, oe-*CAPN1* exacerbated the effects of DEX and reversed the regulatory impact of CAST ($p < 0.05$).

Conclusion: DEX inhibits osteogenic differentiation and reduces ATP activity in BMSCs by modulating the CAST-CAPN1 axis.

Keywords: osteoporosis; osteogenic differentiation; dexamethasone; calpastatin-calpain 1-ATP synthase F1 subunit alpha

Introduction

Osteoporosis is a common systemic metabolic disease characterized by osteopenia and microstructural destruction of bone tissue, leading to increased bone fragility and an increased risk of fractures [1]. The aging population, especially postmenopausal osteoporosis, is gradually rising, exerting an increasing impact on both medicine and society [2]. Moreover, long-term use of glucocorticoids (such as dexamethasone (DEX)) causes up to 20% of osteoporosis cases [3]. Therefore, there is an urgent need to investigate the underlying mechanism of osteoporosis. After a comprehensive analysis of the single-cell sequencing data and related studies from the Origin of Bone and Cartilage Disease (OBCD) database [4,5], we identified some genes linked to bone structure and function. Among these genes, Adenosine triphosphate (ATP) synthase, H+transporting, mitochondrial F1 complex, alpha subunit 1 (*ATP5A1*) emerged as a gene of particular interest.

ATP5A1 is one of the key components of Adenosine triphosphate (ATP), encoding the α subunit of the ATP synthase complex [6]. This subunit is crucial in ATP production by converting adenosine diphosphate (ADP) and inorganic phosphate (pi) into ATP [7]. Research has shown that the expression of ATP5A1 is inhibited in DEX-induced osteoblasts [8]. Mitochondria are dynamic organelles with the most complex sensory systems in cells [9]. Mitochondrial function activation is essential for osteogenic differentiation, a key process in bone formation [10]. Therefore, this study explored the potential role of ATP5A1 in osteoporosis through the perspective of mitochondrial activity.

Bone marrow mesenchymal stem cells (BMSCs) are stem cells derived from mesoderm with multi-directional differentiation potential and are the most abundantly observed in bone marrow tissues [11]. As the key precursor of osteoblasts, impaired osteogenic differentiation and enhanced adipogenic differentiation significantly contribute

to osteoporosis [11,12]. Therefore, in this study, rat BMSCs were used as the research model and an *in vitro* osteoporosis model was established utilizing DEX. Further elucidation demonstrated that changes in ATP5A1 levels may be associated with the calpain system. Moreover, mitochondrial calpain 1 (CAPN1) is associated with reduced ATP5A1 protein levels and ATP synthase activity [13]. Additionally, during osteogenic differentiation, calpain inhibitor levels are elevated [14], whereas DEX has been found to attenuate cytotoxicity triggered by proteasome inhibitors [15]. Furthermore, the protective effects of mitochondrial-targeted calpastatin (CAST) correlate with increased ATP5A1 protein expression and improved ATP synthase activity in the heart [16].

However, to our knowledge, no previous studies have investigated the effect of the calpain system and ATP5A1 in osteoblast differentiation. Therefore, we propose a novel inference: DEX inhibits osteoblast differentiation by regulating the calpain system to inhibit ATP5A1 expression, providing new insights into the underlying mechanisms of osteoporosis.

Materials and Methods

BMSCs Culture

The rat BMSCs (product number: CP-R131, Procell, Wuhan, China) were obtained and properly cultured following the protocol provided in the product manual. BMSCs showed diverse morphologies, including oval, round, bipolar, and large, flat cells. Immunofluorescence analysis using CD90 or CD44 showed more than 90% BMSC purity. Similarly, mycoplasma testing yielded negative results, and morphologically, the cells demonstrated a fibroblast-like appearance. Furthermore, the cells were cultured in BMSCs complete medium (Cat. No. CM-R131, Procell, Wuhan, China), supplemented with 10% fetal bovine serum (Cat. No. 164210, Procell, Wuhan, China) and 1% penicillin-streptomycin solution (Cat. No. PB180120, Procell, Wuhan, China). Moreover, the cell cultures were maintained at 37 °C in an atmosphere of 95% air and 5% CO_2. Before subsequent experimentations, the cells were passaged for at least three generations. The morphological characteristics of BMSCs were examined employing optical microscopy (Leica SP2, Leica Optical Co. Ltd., Wetzlar, Germany).

Treatment of BMSCs

The *in vitro* osteoporosis model was developed using DEX (HY-14648, MCE, Monmouth, NJ, USA) following a previously published protocol [17]. BMSCs were seeded in 35 mm Petri dishes at a density of 1×10^4 cells per plate. The dulbeccos modified eagle medium (DMEM) medium was supplemented with 10 mM β-Glycerophosphate (ST637, Beyotime, Shanghai, China) and 50 µg/mL ascorbate acid (HY-B0166, MCE, Monmouth, NJ, USA). To assess the impact of DEX, different concentrations (0, 1, 10, 20, and 40 nM) were added to the medium. The cell cultures, containing 5% CO_2, were maintained at 37 °C and incubated for 14 days before subsequent experimentations. Moreover, 20 nM DEX were chosen to demonstrate the temporal effects of DEX by time-course experiments. For time-course experiments, aliquots were taken at the indicated time points, BMSCs were intervened with 20 nM DEX and cultured at 37 °C (containing 5% CO_2) for 0, 4, 8, 12 days and collected for subsequent experiments.

The full-length sequences of *CAST* and *CAPN1* were cloned into pcDNA3.1(+) vector (HG-VPI0001, Honorgene, Changsha, China) to construct overexpressed *CAST* (oe-*CAST*) and *CAPN1* (oe-*CAPN1*) plasmids. The empty vector was used as a negative control (NC) for the study. After this, 500 ng oe-*CAST* or oe-*CAPN1* plasmids were transfected into 1.3×10^5 BMSCs in 24-well plates using a Lipofectamine 3000 kit (L3000-008, Invitrogen, Carlsbad, CA, USA). After achieving an 80–90% cell confluence, Opti-minimal essential medium (MEM) media (25 µL) was added to an eppendorf tube along with 1.5 µL Lipofectamine 3000 transfection reagents. In another eppendorf tube, Opti-MEM media (25 µL) was mixed with P3000 reagents (1 µL) and either oe-*CAST* or oe-*CAPN1* plasmids (0.5 µL). The contents of these two tubes were gently mixed, and the 50 µL mixture was added to the BMSCs. After 48 hours, the transfection efficiency of the plasmids was detected using quantitative reverse transcription polymerase chain reaction (qRT-PCR). The untreated group of cells was used as the Blank or Control group. However, the NC group was transfected with an empty vector.

Real Time-Polymerase Chain Reaction

Total RNA was isolated from BMSCs utilizing the TRIeasy™ Total RNA Extraction Reagent (Product No. 10606ES60, YEASEN, Shanghai, China). After quantification, total RNA was converted into cDNA using the HyperScript First-Strand cDNA Synthesis Kit (Catalog No. K1072, APExBIO Technology LLC, Houston, TX, USA). A list of primers (Sangon, Shanghai, China) used in this study is shown in Table 1. Amplification was performed in the real-time PCR detector (ABI 7500, Applied Biosystems, Irvine, CA, USA) using SYBR Green qPCR Master Mix (Catalog No. K1070, APExBIO Technology LLC, Houston, TX, USA). Finally, relative mRNA levels were assessed using the $2^{-\Delta\Delta CT}$ method. The glyceraldehyde-3-phosphate dehydrogenase (*GAPDH*) served as an internal control.

Western Blotting

Total protein was extracted from the transfected or drug-treated BMSCs using high-efficiency radioimmunoprecipitation assay (RIPA) lysis buffer (tissue/cell; product number: R0010, Solarbio LIFE SCIENCES, Bei-

Table 1. A list of primers used in qRT-PCR.

Genes	Forward primer (5′-3′)	Reverse primer (5′-3′)
CAST	CCTGAGCAGAGGGCGTTAAA	AAATTGTACGGGAGGCCCAG
CAPN1	AAACTCCCCTTCCCCAGGAT	AAACTGGAGGGAAGGCATCG
ATP5A1	TACCTACACTCTCGCCTGCT	TACCTACACTCTCGCCTGCT
RUNX2	ACAACTAAAACAGGGACTGGGT	TTGAACCTGGCCACTTGGTT
ALP	GGACGGTGAACGGGAGAA	CCTCAGAACAGGGTGCGTAG
OPN	CCCGGTGAAAGTGACTGATT	AGGTCCTCATCTGTGGCATC
GAPDH	TGTGGGCATCAATGGATTTGG	ACACCATGTATTCCGGGTCAAT

qRT-PCR, quantitative reverse transcription polymerase chain reaction; *CAST*, calpastatin; *CAPN1*, calpain 1; *ATP5A1*, Adenosine triphosphate (ATP) synthase, H+transporting, mitochondrial F1 complex, alpha subunit 1; *RUNX2*, Runt-Related Transcription Factor 2; *ALP*, alkaline phosphatase; *OPN*, osteopontin; *GAPDH*, glyceraldehyde-3-phosphate dehydrogenase.

Table 2. The primary and secondary antibodies are used in Western blotting analysis.

Antibodies	Dilution ratio	Molecular weight	Purchase information
RUNX2	1/1000	52 kDa	ab76956, Abcam, Hercules, CA, USA
ALP	1/800	62 kDa	sc-271431, SantaCruz, Dallas, TX, USA
OPN	1/1000	30 kDa	ab63856, Abcam, Hercules, CA, USA
CAST	1/1000	62 kDa	ab28252, Abcam, Hercules, CA, USA
CAPN1	1/2000	82 kDa	ab108400, Abcam, Hercules, CA, USA
ATP5A1	1/3000	62 kDa	ab176569, Abcam, Hercules, CA, USA
GAPDH	1/10,000	33 kDa	#5174, CST, Boston, MA, USA
Anti-rabbit IgG	1/5000	—	#7074, CST, Boston, MA, USA
Goat anti-mouse IgG (H&L)-HRP	1/5000	—	ab6789, Abcam, Hercules, CA, USA

HRP, Horseradish peroxidase.

jing, China). After quantification, the protein samples were denatured at high temperature. After sodium dodecyl sulfate-polyacrylamide gel electrophoresis (P0690, BioTeke, Shanghai, China), protein samples were transferred onto the polyvinylidene fluoride (PVDF) membrane (IEVH85R, Millipore, Billerica, MA, USA). To block the hydrophobic binding sites on the membrane, the membranes were soaked in a blocking solution for 2 hours. The PVDF membrane underwent overnight incubation at 4 °C with primary antibodies. The following day, the PVDF membrane was incubated with labeled secondary antibody for 1 hour at room temperature. In the next step, enhanced chemiluminescence (ECL) luminescent solution (WBKLS0500, Millipore, Billerica, MA, USA) was applied, and protein bands were visualized using the Tanon-2500 automatic digital gel image analysis system. Relative protein levels were assessed as the ratio of target protein to internal reference GAPDH. A list of antibodies and their dilutions are detailed in Table 2.

ATP Activity Detection

ATP activity in BMSCs was determined using an ATP kit (Cat. No. JN4749, Jining Shiye, Shanghai, China). Transfected or drug-treated BMSCs were washed, and the supernatant was collected. After this, BMSCs, a standard substance, and an Horseradish peroxidase (HRP)-labeled detection antibody were sequentially added to the enzyme-linked immunosorbent assay (ELISA) plate, following the manufacturer's instructions. After terminating the reaction, the plates were analyzed using a microplate reader (HBS-1096C, DeTie, Nanjing, China) at an absorbance wavelength of 450 nm. The ATP activity was assessed using the following formula: ATP activity (%) = (optical delnsity (OD) of determination group – OD of the control group)/OD of the standard group × standard sample concentration × sample dilution × reaction time/protein content × 100%.

Alizarin Red S (ARS) Staining

Transfected or drug-treated BMSCs were fixed with paraformaldehyde (P0099, Beyotime, Shanghai, China) for 10 minutes. After the rinse water was completely removed, the BMSCs were stained with ARS reagent (Cat. No. G1452, Solarbio LIFE SCIENCES, Beijing, China) for 20 minutes. Finally, the staining results were observed under a microscope (LV100ND, Nikon, Tokyo, Japan) at 200× magnification.

Statistical Analysis

Statistical analysis was performed using GraphPad Prism 8.0 (GraphPad Software, Inc., San Diego, CA, USA).

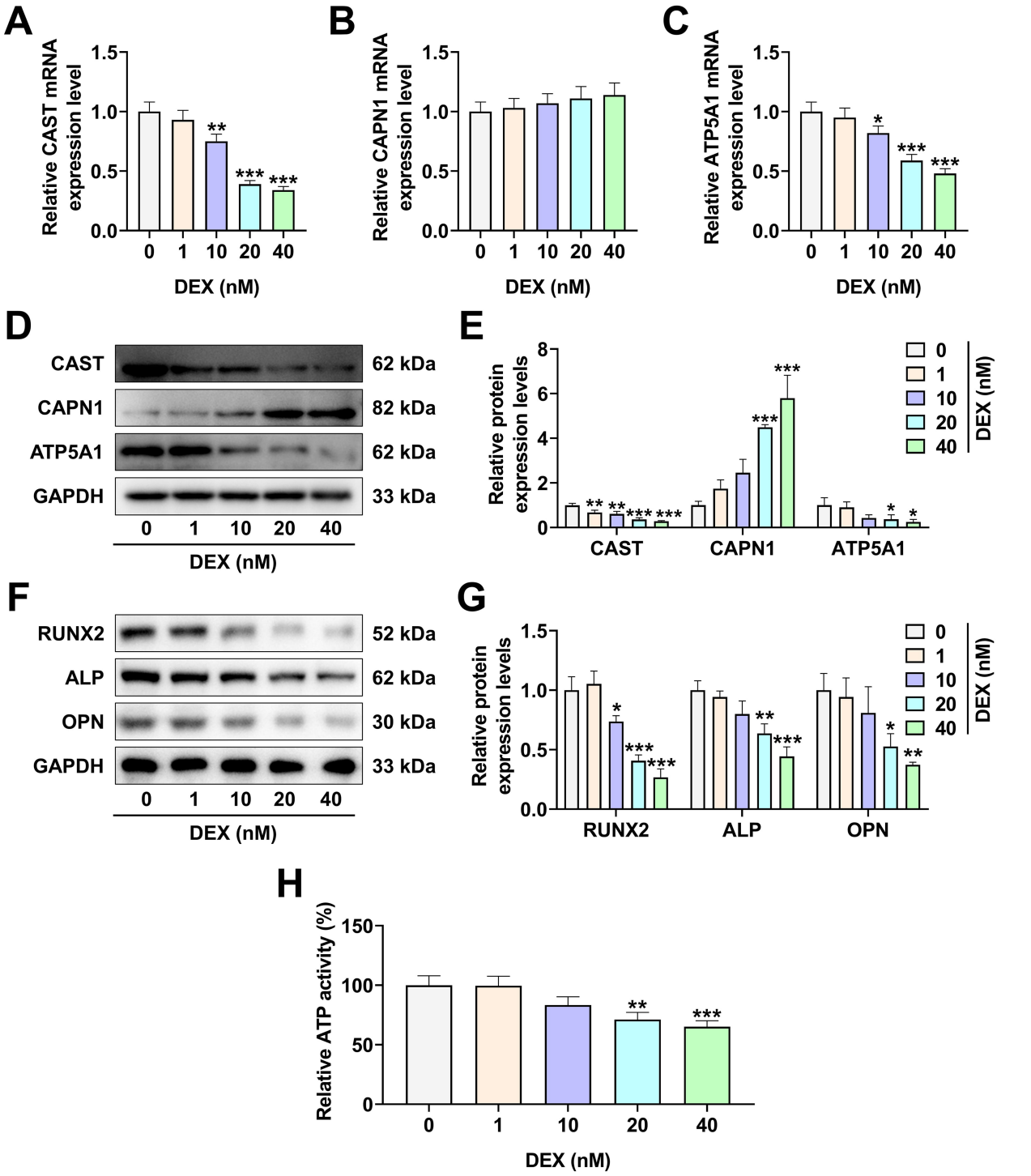

Fig. 1. DEX inhibited the osteogenic differentiation and ATP activity of BMSCs and reduced CAST and ATP5A1 protein expression levels while promoting CAPN1 protein expression levels in a concentration-dependent manner. (A–C) The effects of different concentrations of DEX on *CAST*, *CAPN1* and *ATP5A1* mRNA levels were assessed using qRT-PCR. (D,E) The effects of different concentrations of DEX on CAST, CAPN1 and ATP5A1 protein levels were determined using Western blotting analysis. (F,G) The effects of different concentrations of DEX on osteogenic differentiation marker proteins were evaluated using Western blotting analysis. (H) The effects of different concentrations of DEX on ATP activity in BMSCs were examined using corresponding ELISA kits. *GAPDH* served as an internal reference gene in qRT-PCR and Western blotting analyses. Each experiment was repeated three times. $^{*}p < 0.05$, $^{**}p < 0.01$, $^{***}p < 0.001$ vs. 0 nM. n = 3. DEX treatment: DEX at 0, 1, 10, 20, and 40 nM was added to BMSCs medium and incubated for 14 days. Abbreviations: DEX, dexamethasone; BMSCs, bone marrow mesenchymal stem cells; ELISA, enzyme-linked immunosorbent assay.

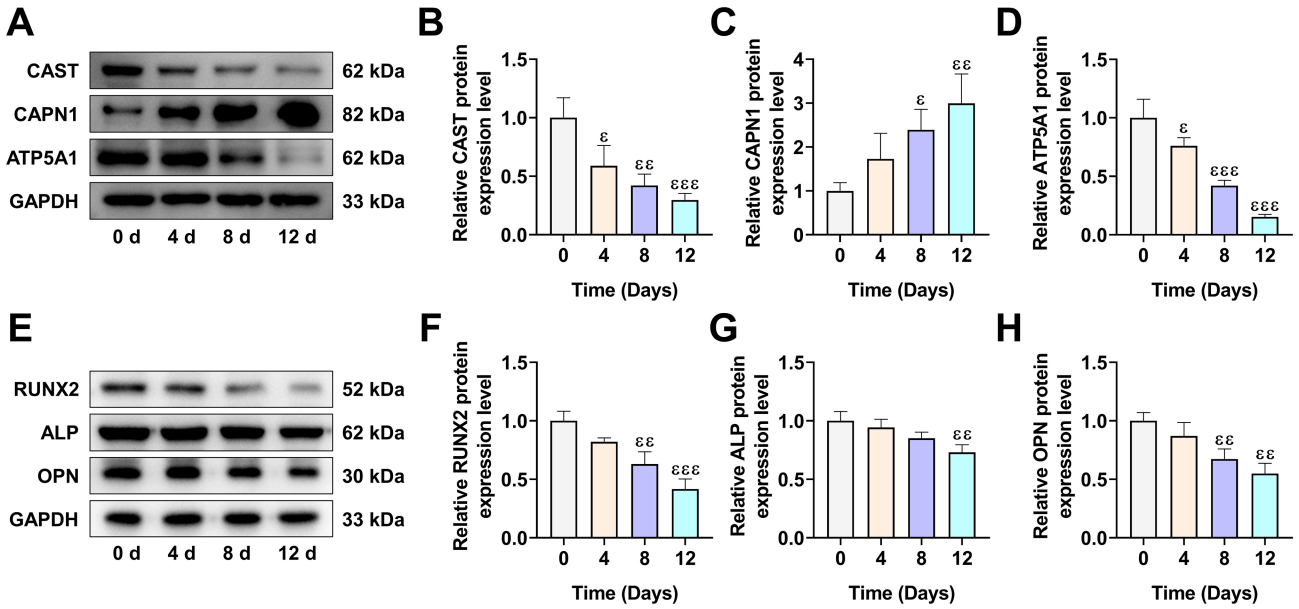

Fig. 2. DEX inhibited the osteogenic differentiation and reduced CAST and ATP5A1 expression while promoting CAPN1 expression in a time-dependent manner. (A–D) The effects of different concentrations of DEX on CAST, CAPN1 and ATP5A1 protein levels were assessed using Western blotting analysis. (E–H) The effects of different concentrations of DEX on osteogenic differentiation marker proteins were determined using Western blotting analysis. $^{\varepsilon}p < 0.05$, $^{\varepsilon\varepsilon}p < 0.01$, $^{\varepsilon\varepsilon\varepsilon}p < 0.001$ vs. 0 d. n = 3.

Measurement data were expressed as mean ± standard deviation. Differences among multiple groups were assessed using one-way analysis of variance (ANOVA), followed by Bonferroni post hoc tests. A p-value of <0.05 was considered statistically significant.

Results

DEX Reduced CAST and ATP5A1 Protein Expression While Increasing CAPN1 Expression

This study successfully established an *in vitro* osteoporotic injury model using the DEX induction method. qRT-PCR analysis (Fig. 1A–C) revealed that DEX at concentrations $\geq$10 nM significantly decreased the expression of *CAST* and *ATP5A1* in BMSCs ($p < 0.05$), while no significant effect was found on the mRNA level of *CAPN1* ($p > 0.05$). Western blotting analysis (Fig. 1D,E) further demonstrated that DEX treatment at concentrations $>$10 nM significantly decreased *CAST* and *ATP5A1* protein expressions in BMSCs ($p < 0.05$) while upregulating CAPN1 protein levels ($p < 0.05$).

DEX Inhibited the Osteogenic Differentiation and ATP Activity of BMSCs

To evaluate the osteogenic differentiation of BMSCs, the levels of key osteogenic differentiation proteins were determined. As shown in Fig. 1F,G, DEX at concentrations $\geq$20 nM substantially downregulated the expression of Runt-Related Transcription Factor 2 (RUNX2), alkaline phosphatase (ALP), and osteopontin (OPN) proteins ($p <$ 0.05), suggesting that DEX inhibited BMSCs osteogenic differentiation. Furthermore, DEX treatment at concentrations $\geq$20 nM significantly decreased ATP activity in BMSCs ($p < 0.05$, Fig. 1H). These findings indicated that 20 nM DEX provided a more stable intervention effect, hence, this concentration was used for subsequent experiments.

Western blotting analysis determined the impact of DEX (20 nM) treatment duration on the calpain-calpastatin system and ATP5A1 expression. It was observed that increasing treatment duration progressively decreased CAST expression, promoted CAPN1 expression, and significantly reduced ATP5A1 expression (Fig. 2A–D, $p < 0.05$). Moreover, prolonged DEX treatment inhibited the osteogenic differentiation of BMSCs in a time-dependent manner (Fig. 2E–H, $p < 0.05$).

DEX Inhibited the Osteogenic Differentiation and ATP Activity of BMSCs by Regulating CAST

Furthermore, we examined whether DEX effects were mediated through CAST modulation. Transfection efficiency analysis (Fig. 3A) revealed that the constructed oe-*CAST* plasmid significantly upregulated *CAST* levels in BMSCs ($p < 0.05$). Moreover, osteogenic markers analysis (Fig. 3B–F) demonstrated that oe-*CAST* significantly up-elevated the expressions of RUNX2, ALP, and OPN in BMSCs, both at mRNA and protein levels ($p < 0.05$), and partially counteracted the inhibitory effect of DEX on their expression ($p < 0.05$). ARS staining further verified these effects on osteogenic marker levels. As illustrated in Fig. 3G,H, the calcium deposition increased in the

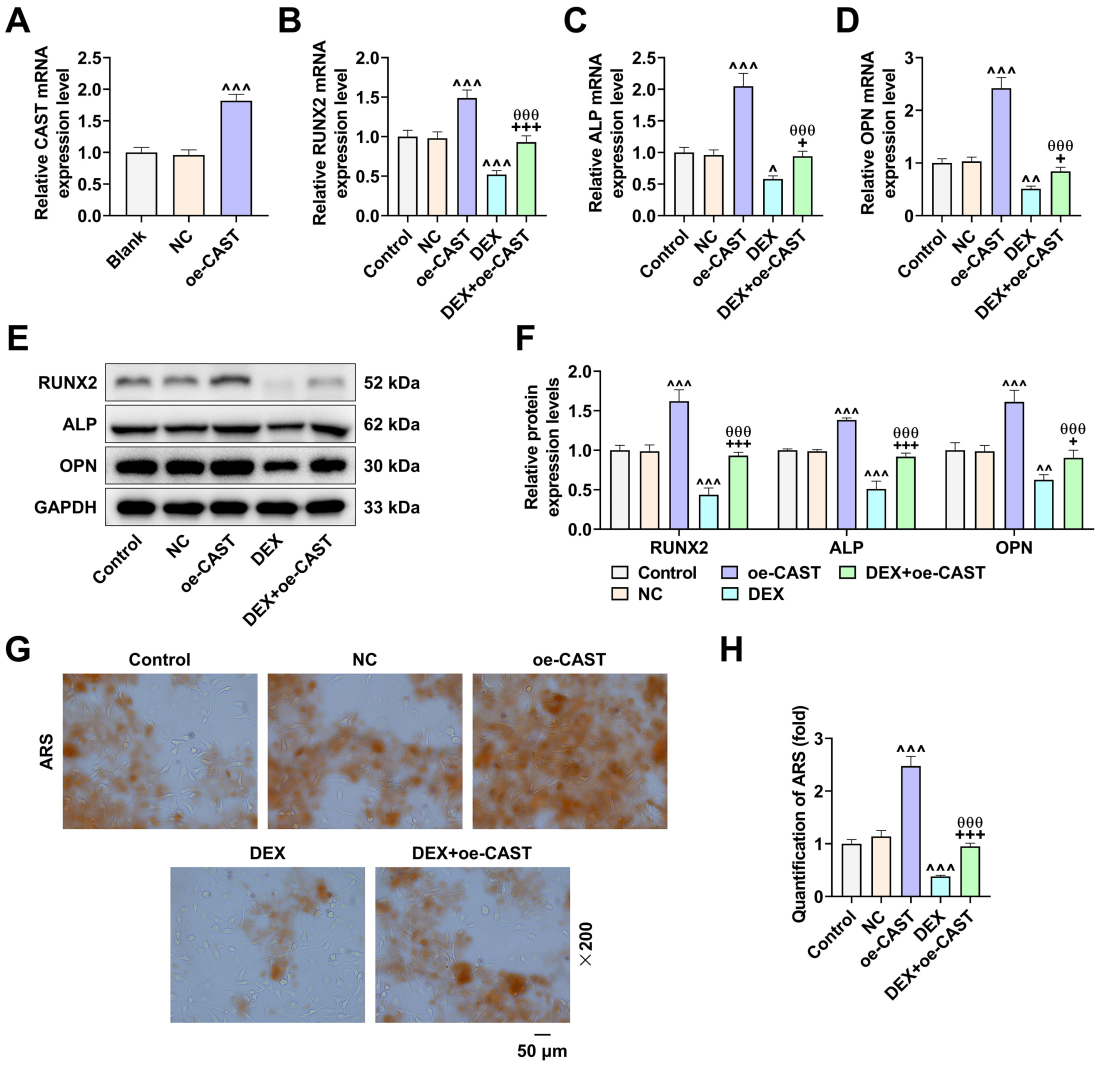

Fig. 3. oe-*CAST* partially counteracted the inhibitory effect of DEX on osteogenic differentiation of BMSCs. (A) The transfection efficiency of the oe-*CAST* plasmid was verified using qRT-PCR. (B–D) The effects of oe-*CAST* and *DEX* on mRNA levels of osteogenic differentiation markers were assessed using qRT-PCR. (E,F) The effects of oe-*CAST* and DEX on osteogenic differentiation marker proteins were determined using Western blotting analysis. (G,H) The effects of oe-*CAST* and DEX on the osteogenic differentiation of BMSCs were analyzed using ARS staining. Magnification: 200 times. *GAPDH* served as an internal reference gene in qRT-PCR and Western blotting analyses. Each experiment was repeated three times. $^{\wedge}p < 0.05$, $^{\wedge\wedge}p < 0.01$, $^{\wedge\wedge\wedge}p < 0.001$ vs. NC; $^{+}p < 0.05$, $^{+++}p < 0.001$ vs. DEX; $^{\theta\theta\theta}p < 0.001$ vs. oe-*CAST*. n = 3. DEX treatment: 20 nM DEX was added to the BMSCs medium and incubated for 14 days. Abbreviations: oe-*CAST*, overexpression calpastatin; ARS, Alizarin Red S; NC, negative control.

oe-*CAST* group while significantly decreased in the DEX group ($p < 0.05$). Furthermore, compared to the DEX group, the DEX+oe-*CAST* group showed elevated calcium deposition ($p < 0.05$), suggesting a potential protective impact of CAST against DEX-triggered osteogenic inhibition.

This study further assessed the expression levels of CAST, CAPN1, and ATP5A1 proteins, as well as ATP activity. It was found that oe-*CAST* significantly elevated the expression of CAST and ATP5A1 proteins, upregulated ATP activity in BMSCs, and inhibited CAPN1 protein expression (Fig. 4A–E, $p < 0.05$); oe-*CAST* partially reversed the inhibitory effects of DEX ($p < 0.05$).

DEX Inhibited Osteogenic Differentiation and ATP Activity of BMSCs by Regulating the CAST-CAPN1 Axis

Transfection efficiency analysis demonstrated that the constructed oe-*CAPN1* significantly upregulated *CAPN1* levels in BMSCs (Fig. 5A, $p < 0.05$). The level of osteogenic differentiation showed that oe-*CAPN1* further enhanced the inhibitory effect of DEX on the expression of RUNX2, ALP, and OPN (Fig. 5B–F, $p < 0.05$), as well as reduced calcium deposition in BMSCs (Fig. 5G,H, $p < 0.05$). On the contrary, oe-*CAST* partially counteracted DEX-induced molecular changes (Fig. 5B–F, $p < 0.05$)

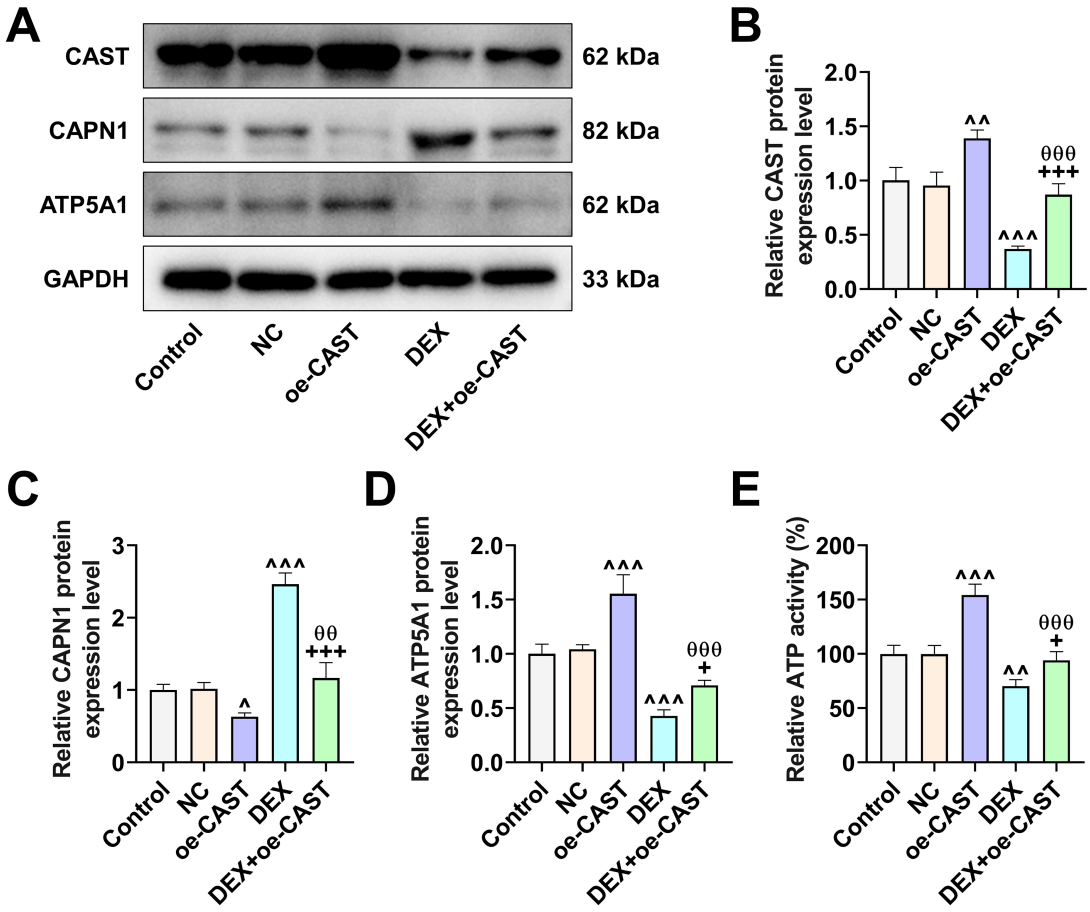

Fig. 4. oe-*CAST* partially counteracted the inhibitory effect of DEX on ATP activity in BMSCs. (A–D) The effects of oe-*CAST* and DEX on CAST, CAPN1, and ATP5A1 proteins were analyzed using Western blotting analysis. (E) The effects of oe-*CAST* and DEX on ATP activity in BMSCs were determined using an ATP kit. *GAPDH* served as an internal reference gene in Western blotting analysis. Each experiment was repeated three times. $^{\wedge}p < 0.05$, $^{\wedge\wedge}p < 0.01$, $^{\wedge\wedge\wedge}p < 0.001$ vs. NC; $^{+}p < 0.05$, $^{+++}p < 0.001$ vs. DEX; $^{\theta\theta}p < 0.01$, $^{\theta\theta\theta}p < 0.001$ vs. oe-CAST. n = 3. DEX treatment: 20 nM of DEX was added to the BMSCs medium and incubated for 14 days.

and promoted calcium deposition (Fig. 5G,H, $p < 0.05$). However, oe-*CAPN1* reversed the effects of CAST in the DEX+oe-*CAST*+oe-*CAPN1* group (Fig. 5B–H, $p < 0.05$).

In evaluating ATP5A1 expression and ATP activity, oe-*CAPN1* further decreased ATP5A1 expression and ATP activity (Fig. 5I–K, $p < 0.05$). Furthermore, oe-*CAPN1* showed a negative regulatory effect (Fig. 5I–K, $p < 0.05$) and, consistent with previous results, reversed the inhibitory effect of CAST on DEX function (Fig. 5I–K, $p < 0.05$).

Discussion

The decreased osteogenic differentiation capability of BMSCs plays a vital role in the occurrence and progression of osteoporosis [18,19]. Therefore, exploring approaches to reduce the effect of interfering factors on the osteogenic differentiation of BMSCs is highly significant for osteoporosis management, ultimately improving the quality of life and well-being of the elderly. Glucocorticoids, like DEX, are widely used in clinical practice, with about 40% of patients who receive long-term glucocorticoid therapy experiencing osteoporosis [20]. Research has shown that glucocorticoids promote osteoclasts production, inhibit osteoblasts production, stimulate apoptosis in osteocytes and osteoblasts, reduce osteocyte numbers, increase bone resorption, and reduce bone density, ultimately resulting in osteoporosis [21,22]. This study used glucocorticoid-induced reduction of osteogenic differentiation to develop an *in vitro* osteoporosis model. After DEX treatment, the osteogenic differentiation process was inhibited, consistent with prior studies. Moreover, ATP5A1 and CAPN1 expression were reduced, and CAST expression was elevated. CAST plays a vital role in normal osteoclast function by constitutively cleaving talin, flamin A, and Pyk2 [23]. CAST is an endogenous protein that specifically inhibits CAPN activity [24]. A previous study showed that mitochondrial CAPN1 activates the nucleotide-binding oligomerization domain-like receptor protein 3 (NLRP3) inflammasome by cleaving ATP5A1 [25]. Based on this observation, we guessed

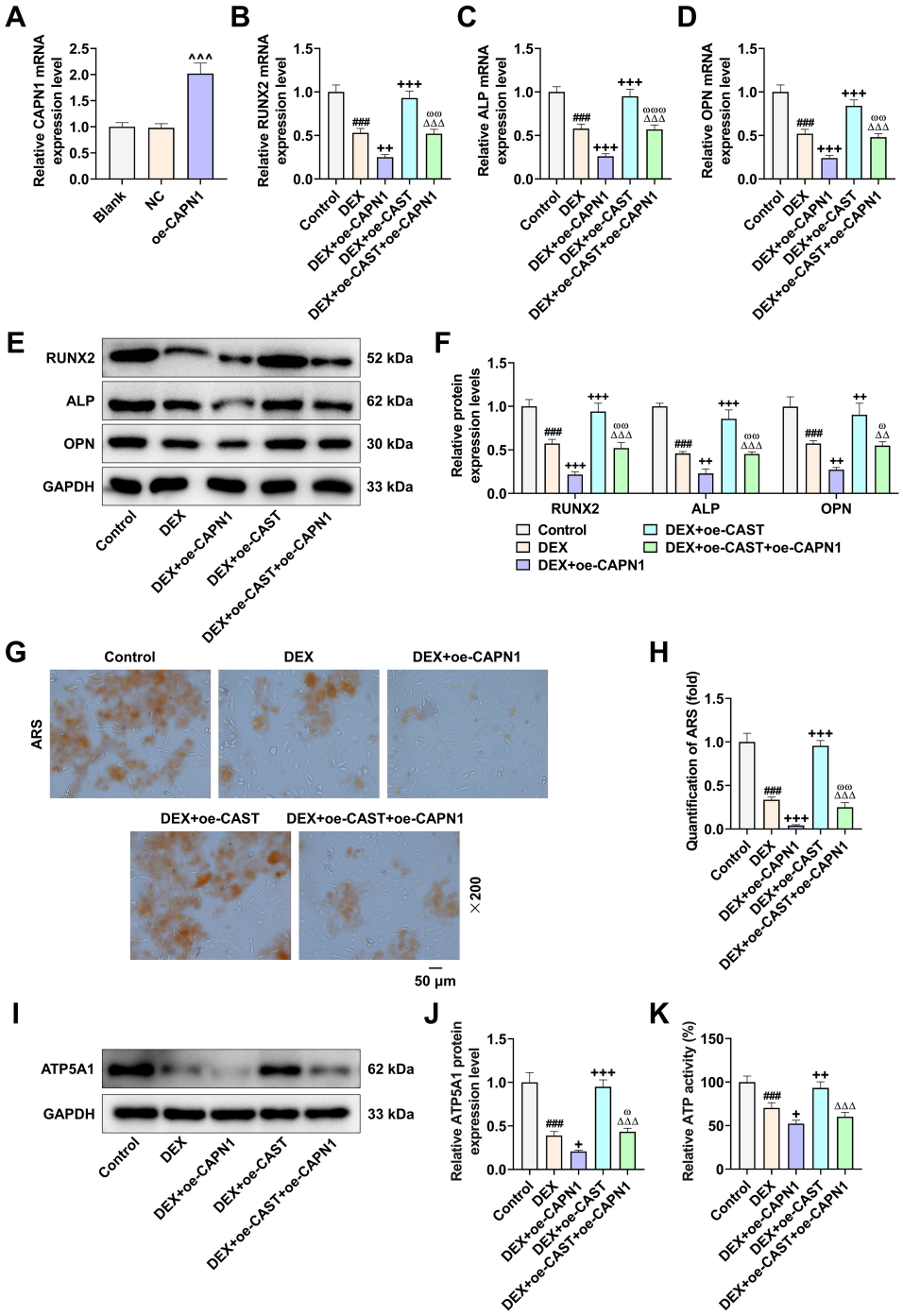

Fig. 5. DEX inhibited osteogenic differentiation and ATP activity of BMSCs by regulating the CAST-CAPN1 axis. (A) The transfection efficiency of oe-*CAPN1* was verified using qRT-PCR. (B–D) The effects of oe-*CAST* and oe-*CAPN1* on mRNA levels of osteogenic differentiation markers were assessed using qRT-PCR. (E,F) The effects of oe-*CAST* and oe-*CAPN1* on osteogenic differentiation marker proteins were determined using Western blotting analysis. (G,H) The impacts of oe-*CAST* and oe-*CAPN1* on the osteogenic differentiation of BMSCs were analyzed through ARS staining. Magnification: 200×. (I,J) The effects of oe-*CAST* and oe-*CAPN1* on ATP5A1 protein were determined using Western blotting analysis. (K) The impacts of oe-*CAST* and oe-*CAPN1* on ATP activity in BMSCs were assessed using an ATP kit. *GAPDH* served as an internal reference gene in qRT-PCR and Western blotting analyses. Each experiment was repeated three times. $^{\wedge\wedge\wedge}p < 0.001$ vs. NC; $^{\#\#\#}p < 0.001$ vs. Control; $^{+}p < 0.05$, $^{++}p < 0.01$, $^{+++}p < 0.001$ vs. DEX; $^{\Delta}p < 0.05$, $^{\Delta\Delta}p < 0.01$, $^{\Delta\Delta\Delta}p < 0.001$ vs. DEX+oe-CAST; $^{\omega}p < 0.05$, $^{\omega\omega}p < 0.01$, $^{\omega\omega\omega}p < 0.001$ vs. DEX+oe-CAPN1. n = 3. DEX treatment: 20 nM of DEX was added to the BMSCs medium and incubated for 14 days. Abbreviations: oe-CAPN1, overexpressed CAPN1.

that DEX affects ATP5A1 expression by regulating the calpain system. To test this speculation, we designed a rescue experiment focusing on the CAST-CAPN1 core pathway.

The calpain system comprises various calpains (CAPN) and endogenous inhibitory proteins (CAST). CAPN, an intracellular cysteine proteinase, comprises three key molecules, such as Ca^{2+}-dependent neutral proteinases CAPN1 (μ-calpain) and CAPN2 (m-calpain), and their inhibitor CAST, collectively constituting the calpain proteolytic system [26]. They are located in the cytoplasm and coexist with CAPN [27]. In our study, DEX treatment resulted in a downregulation of CAST expression and upregulation of CAPN1, with overexpression of CAPN1 could further enhance the DEX treatment effect. However, overexpression of CAST reversed the effect of both CAPN1 and DEX. Rescue experiments confirmed that DEX inhibited ATP5A1 expression by regulating the CAST-CAPN1 axis.

Combining these findings with the published literature, a reasonable explanation emerges. Under pathological conditions, the concentration of Ca^{2+} in mitochondria is abnormally increased [28,29]. Ca^{2+}-activated CAPN1 accelerates apoptosis [30], while DEX further reduces CAST activity, resulting in promoted CAPN1 activation. This molecular cascade results in decreased ATP5A1 expression, decreased ATP activity, mitochondrial dysfunction, and ultimately hindered the osteogenic differentiation of BMSCs. These results underscore the CAST-CAPN1-ATP5A1 axis as a valuable target for further understanding the mechanisms underlying osteoporosis.

Furthermore, previous research has reported that ATP causes bone cell death and influences the progression of osteoporosis by modulating cell membrane surface receptors, immune-inflammatory responses, and mitochondria-related signaling pathways [31]. However, further investigation is necessary to elucidate the molecular mechanism underlying ATP level alterations and to reveal the specific regulatory pathways involved in osteoporosis. ATP5A1 expression is upregulated, and its activation is linked to mitochondrial ATP synthetase function and ATP synthesis catalysis [32]. Changes in serum levels of specific ATP-related proteins (such as purinergic 2 receptor (P2R)) have been found in osteoporosis and its associated complications, but their specificity remains inadequate for clinical diagnosis [31]. Therefore, ATP5A1 has the potential to be a novel diagnostic marker for osteoporosis, though further experimental confirmation is required.

However, a limitation of the present study is the lack of time-course experiments to demonstrate the temporal effects of DEX on the CAST-CAPN1-ATP5A1 axis and osteogenic differentiation. Moreover, *in vitro* experiments cannot fully mimic the complications of *in vivo* conditions. Additionally, the BMSCs used in this study were not primary cells isolated and cultured from mice or rats, and various cellular responses could impact BMSC behavior. Therefore, in the future, we plan to use primary cells or animal models to further verify the specificity of ATP5A1 in osteoporosis, offering more basic research evidence for potential therapeutic target identification.

Conclusion

With the aging population, the incidence of osteoporosis is increasing year by year. Its severe complication, "fragile fracture", is linked to high disability and fatality rate, significantly affecting the quality of life and physical and overall well-being. Identifying effective approaches to prevent and treat osteoporosis has become a crucial research focus. This study revealed that DEX inhibits the osteogenic differentiation of BMSCs in rats by regulating the CAST-CAPN1-ATP5A1 axis, providing comprehensive insights into the regulatory mechanisms underlying osteogenic differentiation. These observations are crucial for advancing our understanding of the pathogenesis of osteoporosis and expanding treatment options.

Availability of Data and Materials

The analyzed data sets generated during the study are available from the corresponding author upon reasonable request.

Author Contributions

GZ designed the research study; SQC and ZZ performed the research; LT collected and analyzed the data. All authors have been involved in drafting the manuscript and have been involved in revising it critically for important intellectual content. All authors give final approval of the version to be published. All authors participated sufficiently in the work to take public responsibility for appropriate portions of the content and agreed to be accountable for all aspects of the work in ensuring that questions related to its accuracy or integrity.

Ethics Approval and Consent to Participate

Not applicable.

Acknowledgment

Not applicable.

Funding

This work was supported by Chengdu Medical Association Research Project [grant number 2023131].

Conflict of Interest

The authors declare no conflict of interest.

References

[1] Yu Z, Wu Y, Zhang R, Li Y, Zang S, Liu J. Increased risk of non-alcoholic fatty liver disease fibrosis is closely associated with osteoporosis in women but not in men with type 2 diabetes. Endocrine Connections. 2022; 11: e220174.

[2] Yong EL, Logan S. Menopausal osteoporosis: screening, prevention and treatment. Singapore Medical Journal. 2021; 62: 159–166.

[3] Cai Z, Wang H, Jiang J, Xiao S, Xiao J, He J, *et al*. Elaborate the Mechanism of Ancient Classic Prescriptions (Erzhi Formula) in Reversing GIOP by Network Pharmacology Coupled with Zebrafish Verification. Evidence-Based Complementary and Alternative Medicine. 2022; 2022: 7019792.

[4] McDonald MM, Khoo WH, Ng PY, Xiao Y, Zamerli J, Thatcher P, *et al*. Osteoclasts recycle via osteomorphs during RANKL-stimulated bone resorption. Cell. 2021; 184: 1330–1347.e13.

[5] Freudenthal B, Logan J, Sanger Institute Mouse Pipelines, Croucher PI, Williams GR, Bassett JHD. Rapid phenotyping of knockout mice to identify genetic determinants of bone strength. The Journal of Endocrinology. 2016; 231: R31–46.

[6] Yue L, Liu P, Ma N, Xu Y, Zhu C. Interaction between extracellular ATP5A1 and LPS alleviates LPS-induced neuroinflammation in mice. Neuroscience Letters. 2021; 758: 136005.

[7] Pan J, Sun LC, Tao YF, Zhou Z, Du XL, Peng L, *et al*. ATP synthase ecto-α-subunit: a novel therapeutic target for breast cancer. Journal of Translational Medicine. 2011; 9: 211.

[8] Hong D, Chen HX, Yu HQ, Wang C, Deng HT, Lian QQ, *et al*. Quantitative proteomic analysis of dexamethasone-induced effects on osteoblast differentiation, proliferation, and apoptosis in MC3T3-E1 cells using SILAC. Osteoporosis International: a Journal Established as Result of Cooperation between the European Foundation for Osteoporosis and the National Osteoporosis Foundation of the USA. 2011; 22: 2175–2186.

[9] Annesley SJ, Fisher PR. Mitochondria in Health and Disease. Cells. 2019; 8: 680.

[10] Wang J, Gao Z, Gao P. MiR-133b Modulates the Osteoblast Differentiation to Prevent Osteoporosis Via Targeting GNB4. Biochemical Genetics. 2021; 59: 1146–1157.

[11] Arthur A, Gronthos S. Clinical Application of Bone Marrow Mesenchymal Stem/Stromal Cells to Repair Skeletal Tissue. International Journal of Molecular Sciences. 2020; 21: 9759.

[12] Zhou X, Cao H, Guo J, Yuan Y, Ni G. Effects of BMSC-Derived EVs on Bone Metabolism. Pharmaceutics. 2022; 14: 1012.

[13] Ni R, Zheng D, Xiong S, Hill DJ, Sun T, Gardiner RB, *et al*. Mitochondrial Calpain-1 Disrupts ATP Synthase and Induces Superoxide Generation in Type 1 Diabetic Hearts: A Novel Mechanism Contributing to Diabetic Cardiomyopathy. Diabetes. 2016; 65: 255–268.

[14] Yajima Y, Kawashima S. Calpain function in the differentiation of mesenchymal stem cells. Biological Chemistry. 2002; 383: 757–764.

[15] Jannuzzi AT, Korkmaz NS, Gunaydin Akyildiz A, Arslan Eseryel S, Karademir Yilmaz B, Alpertunga B. Molecular Cardiotoxic Effects of Proteasome Inhibitors Carfilzomib and Ixazomib and Their Combination with Dexamethasone Involve Mitochondrial Dysregulation. Cardiovascular Toxicology. 2023; 23: 121–131.

[16] Zheng D, Cao T, Zhang LL, Fan GC, Qiu J, Peng TQ. Targeted inhibition of calpain in mitochondria alleviates oxidative stress-induced myocardial injury. Acta Pharmacologica Sinica. 2021; 42: 909–920.

[17] He HP, Gu S. The PPAR-γ/SFRP5/Wnt/β-catenin signal axis regulates the dexamethasone-induced osteoporosis. Cytokine. 2021; 143: 155488.

[18] Ma Y, Qi M, An Y, Zhang L, Yang R, Doro DH, *et al*. Autophagy controls mesenchymal stem cell properties and senescence during bone aging. Aging Cell. 2018; 17: e12709.

[19] Qi M, Zhang L, Ma Y, Shuai Y, Li L, Luo K, *et al*. Autophagy Maintains the Function of Bone Marrow Mesenchymal Stem Cells to Prevent Estrogen Deficiency-Induced Osteoporosis. Theranostics. 2017; 7: 4498–4516.

[20] Yao XW, Liu ZY, Ma NF, Jiang WK, Zhou Z, Chen B, *et al*. Exosomes from Adipose-Derived Stem Cells Alleviate Dexamethasone-Induced Bone Loss by Regulating the Nrf2/HO-1 Axis. Oxidative Medicine and Cellular Longevity. 2023; 2023: 3602962.

[21] Compston J. Glucocorticoid-induced osteoporosis: an update. Endocrine. 2018; 61: 7–16.

[22] Lane NE. Glucocorticoid-Induced Osteoporosis: New Insights into the Pathophysiology and Treatments. Current Osteoporosis Reports. 2019; 17: 1–7.

[23] Wang JW, Yeh CB, Chou SJ, Lu KC, Chu TH, Chen WY, *et al*. YC-1 alleviates bone loss in ovariectomized rats by inhibiting bone resorption and inducing extrinsic apoptosis in osteoclasts. Journal of Bone and Mineral Metabolism. 2018; 36: 508–518.

[24] Stillger MN, Chen CY, Lai ZW, Li M, Schäfer A, Pagenstecher A, *et al*. Changes in calpain-2 expression during glioblastoma progression predisposes tumor cells to temozolomide resistance by minimizing DNA damage and p53-dependent apoptosis. Cancer Cell International. 2023; 23: 49.

[25] Liu X, Li M, Chen Z, Yu Y, Shi H, Yu Y, *et al*. Mitochondrial calpain-1 activates NLRP3 inflammasome by cleaving ATP5A1 and inducing mitochondrial ROS in CVB3-induced myocarditis. Basic Research in Cardiology. 2022; 117: 40.

[26] Nian H, Ma B. Calpain-calpastatin system and cancer progression. Biological Reviews of the Cambridge Philosophical Society. 2021; 96: 961–975.

[27] Chen Y, Su Z, Liu F. Effects of functionally diverse calpain system on immune cells. Immunologic Research. 2021; 69: 8–17.

[28] Luan G, Li G, Ma X, Jin Y, Hu N, Li J, *et al*. Dexamethasone-Induced Mitochondrial Dysfunction and Insulin Resistance-Study in 3T3-L1 Adipocytes and Mitochondria Isolated from Mouse Liver. Molecules. 2019; 24: 1982.

[29] Liu J, Peng Y, Wang X, Fan Y, Qin C, Shi L, *et al*. Mitochondrial Dysfunction Launches Dexamethasone-Induced Skeletal Muscle Atrophy via AMPK/FOXO3 Signaling. Molecular Pharmaceutics. 2016; 13: 73–84.

[30] Chelko SP, Keceli G, Carpi A, Doti N, Agrimi J, Asimaki A, *et al*. Exercise triggers CAPN1-mediated AIF truncation, inducing myocyte cell death in arrhythmogenic cardiomyopathy. Science Translational Medicine. 2021; 13: eabf0891.

[31] Wang W, Zhang H, Sandai D, Zhao R, Bai J, Wang Y, *et al*. ATP-induced cell death: a novel hypothesis for osteoporosis. Frontiers in Cell and Developmental Biology. 2023; 11: 1324213.

[32] Saquib Q, Al-Salem AM, Siddiqui MA, Ansari SM, Zhang X, Al-Khedhairy AA. Cyto-Genotoxic and Transcriptomic Alterations in Human Liver Cells by Tris (2-Ethylhexyl) Phosphate (TEHP): A Putative Hepatocarcinogen. International Journal of Molecular Sciences. 2022; 23: 3998.